

Ambipolar transport behavior in In₂O₃/pentacene hybrid heterostructure and their complementary circuits

Dhananjay, Chun-Wei Ou, Chuan-Yi Yang, Meng-Chyi Wu, and Chih-Wei Chu

Citation: *Applied Physics Letters* **93**, 033306 (2008); doi: 10.1063/1.2949872

View online: <http://dx.doi.org/10.1063/1.2949872>

View Table of Contents: <http://scitation.aip.org/content/aip/journal/apl/93/3?ver=pdfcov>

Published by the [AIP Publishing](#)

Articles you may be interested in

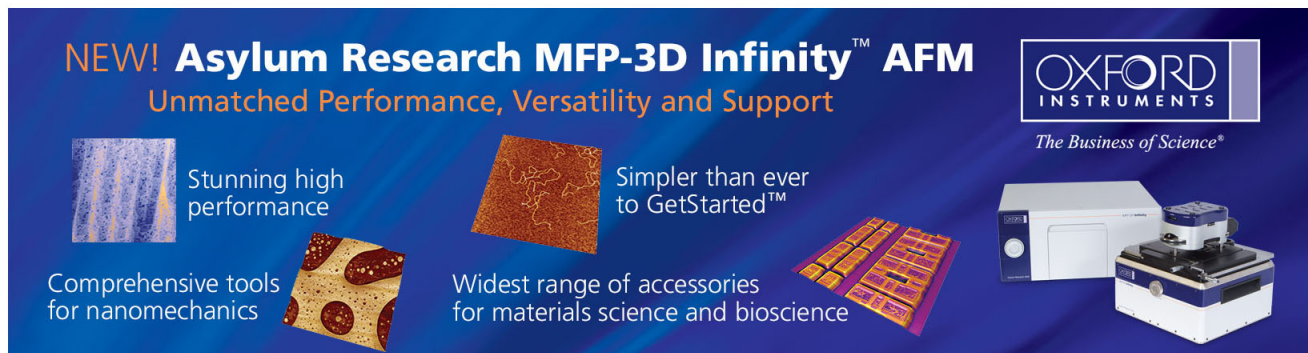
Trap elimination and injection switching at organic field effect transistor by inserting an alkane (C₄₄H₉₀) layer
Appl. Phys. Lett. **90**, 033504 (2007); 10.1063/1.2431713

Modification of the electric conduction at the pentacene/SiO₂ interface by surface termination of SiO₂
Appl. Phys. Lett. **86**, 103502 (2005); 10.1063/1.1875749

Fabrication of ambipolar field-effect transistor device with heterostructure of C₆₀ and pentacene
Appl. Phys. Lett. **85**, 4765 (2004); 10.1063/1.1818336

Effects of FeCl₃ doping on polymer-based thin film transistors
J. Appl. Phys. **96**, 454 (2004); 10.1063/1.1760838

Effects of substrate temperature on the device properties of pentacene-based thin film transistors using Al₂O_{3+x} gate dielectric
J. Appl. Phys. **95**, 3733 (2004); 10.1063/1.1650886

The advertisement features a dark blue background with white and orange text. At the top left, it reads 'NEW! Asylum Research MFP-3D Infinity™ AFM' in large white letters, followed by 'Unmatched Performance, Versatility and Support' in orange. To the right is the Oxford Instruments logo, which includes the text 'OXFORD INSTRUMENTS' and the tagline 'The Business of Science®'. Below the text are several images: a textured surface, a grid of small squares, and a photograph of the MFP-3D Infinity AFM instrument. Text blocks describe the instrument's capabilities: 'Stunning high performance', 'Simpler than ever to GetStarted™', 'Comprehensive tools for nanomechanics', and 'Widest range of accessories for materials science and bioscience'.

Ambipolar transport behavior in In₂O₃/pentacene hybrid heterostructure and their complementary circuits

Dhananjay,¹ Chun-Wei Ou,² Chuan-Yi Yang,² Meng-Chyi Wu,² and Chih-Wei Chu^{1,3,a)}

¹Research Center for Applied Sciences, Academia Sinica, Taipei 11529, Taiwan

²Department of Electrical Engineering, National Tsing Hua University, Hsinchu 30013, Taiwan

³Department of Photonics, National Chiao-Tung University, Hsinchu 30013, Taiwan

(Received 28 April 2008; accepted 2 June 2008; published online 21 July 2008)

In this Letter, ambipolar transport properties of a bilayer of In₂O₃ and a pentacene heterostructure have been realized. While In₂O₃ thin film transistors exhibited a *n*-channel behavior, pentacene presumed *p*-channel characteristics on bare SiO₂/*p*-Si substrates. However, when a bilayer of In₂O₃/pentacene was realized on the gate dielectrics, the hybrid structure exhibited both *n*- and *p*-channel conduction, depicting an ambipolar transistor behavior. When two identical ambipolar transistors were integrated to establish an inverter structure, a voltage gain of 10 was obtained. The results indicate that these heterostructures can be utilized for the complementary circuits. © 2008 American Institute of Physics. [DOI: 10.1063/1.2949872]

Recent technological developments in the area of ambipolar transistors generate an enormous demand for a variety of materials. These ambipolar transistors, when used in complementary metal oxide semiconductor (CMOS) circuits, simplifies the circuit design since a single device can operate both as *p*- and *n*-channel transistors.^{1,2} Progressing in this direction, there are numerous reports available in the literature, especially on the organic ambipolar thin film transistors (TFTs) realized in a wide variety of structures.^{3,4} There are many ways by which they were realized. Conventionally, they are prepared by a process of blending the *n* and *p* organic semiconductors⁵ or by a bilayer structure.⁶ In addition to the routine planar type ambipolar TFTs,⁷ they have also been achieved in a vertical configuration and such results are reported in a literature.⁸ In recent years, hybrid technology comprising of organic and inorganic components has attracted a great deal of interest because of their superior structural and transport properties compared to their individual components. Organic thin films such as pentacene are widely studied as active channel layers for the TFTs.⁹ Like most of the *p*-type organic semiconductors studied, pentacene exhibits inherent *p*-type conduction when grown on a SiO₂ gate oxide. On the other hand, metal oxide systems such as indium oxide (In₂O₃) were found to be promising materials for the *n*-channel TFTs.¹⁰ The *n*-type behavior could largely be attributed to the oxygen vacancies and the metal ion interstitials. Integration of *p*- and *n*-channel materials to realize ambipolar transport in these systems could be much more interesting because the implementation of such ambipolar transistors could make the design of the logic circuits simple and hence result in an easy fabrication process. Hence, the fabrication of hybrid TFTs based on an In₂O₃/pentacene heterostructure was carried out and their performance was studied through the conventional output and transfer curves. They were also employed for the fabrication of complementary inverters, and the data are presented herein.

A heavily *n*-doped Si substrate acts as a gate electrode with a thermally grown 300 nm SiO₂ layer as a gate dielec-

tric. The first layer of the heterostructure, namely, In₂O₃, was deposited by a reactive evaporation process using indium as an evaporation source and oxygen as a reactive gas. During deposition the substrate temperature was set at 100 °C and the deposition was carried out at a pressure of 1.6 × 10⁻⁴ Torr. The first layer thickness plays a major role in achieving ambipolar transport behavior in heterostructure devices. Film thickness and deposition rates were monitored using a quartz crystal monitor. The critical parameter in obtaining the ambipolar behavior in the heterostructure of In₂O₃/pentacene was found to be the thickness and morphology of In₂O₃ layer. The critical thickness of the In₂O₃ thin films for the realization of the ambipolar behavior was 3 nm. After the deposition, the films were subjected to air annealing at 750 °C for 1 h to get the desired TFT properties. The films were then transferred to a vacuum chamber to deposit pentacene through a shadow mask. The thickness of the pentacene layer was fixed at 20 nm and the deposition rate was less than 0.5 Å/s. Finally, Au source/drain electrodes of approximately 50 nm thickness were vacuum deposited through a shadow mask with a channel width of 2 mm and a length of 100 μm. The surface morphology of the individual layers was observed through atomic force microscopy. The output and transfer characteristics of the devices were measured with an Agilent 4156 semiconductor parameter analyzer. To form an inverter, two ambipolar TFTs fabricated under similar conditions were combined. All the measurements were carried out at room temperature and in a glove-box filled with nitrogen.

Initially, optimization of the In₂O₃ layer thickness for the hybrid ambipolar TFTs was carried out. During the optimization process, the thickness of the films was varied and their morphology together with the transport properties was analyzed. Figure 1 shows the atomic force microscope atomic force microscope (AFM) images of In₂O₃ thin films with thicknesses of 3, 5, 7, and 10 nm grown on a SiO₂ gate dielectric. As observed from Fig. 1, both grain size and the root-mean-square roughness were found to be a strong function of thickness of the films and found to increase with the increase in thickness. A quantitative examination of the AFM images revealed that the surface roughness of the

a) Author to whom all correspondence should be addressed. Electronic mail: gchu@gate.sinica.edu.tw.

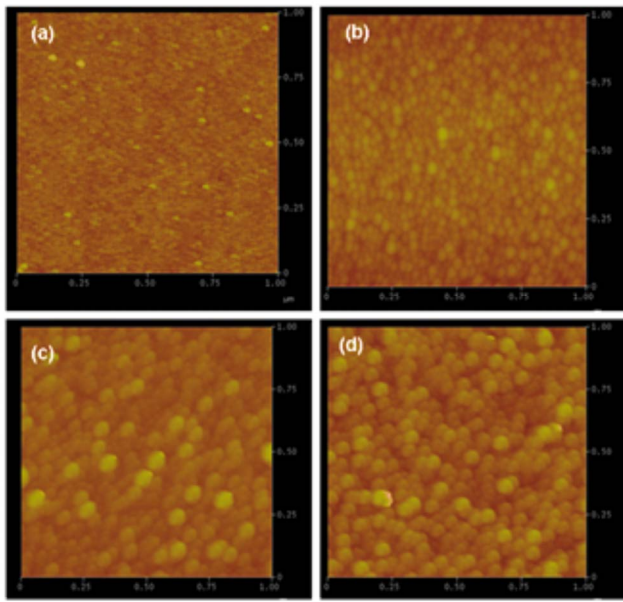


FIG. 1. (Color online) AFM images of In_2O_3 thin films of varying thicknesses: (a) 3 nm, (b) 5 nm, (c) 7 nm, and (d) 10 nm.

In_2O_3 thin films are 0.3, 1.3, 2.8, and 3.2 nm for the film thicknesses of 3, 5, 7, and 10 nm, respectively. The surface morphology of films with a thickness of 3 nm was found to be suitable for the growth of the ambipolar devices mainly due to its minimal surface roughness. Such a minimum surface roughness ensures a favored growth for the pentacene films. Moreover, the balanced electron and hole transport is essential and necessary for the realization of ambipolar conduction. Even though the films with thicknesses below 3 nm exhibited better surface morphology compared to that of 3 nm films, their mobility is far below the value required for the balanced charge transport. Such thickness dependent phenomena in In_2O_3 TFTs were reported previously¹¹ and hence, for the successful observation of the ambipolar transport in the In_2O_3 /pentacene heterostructure, the thickness of 3 nm for In_2O_3 thin films was found to be optimum. Subsequently, the films were processed for the pentacene deposition, which serve as a p -type conductor for these heterostructures.

Figure 2 shows the drain-current-drain voltage (I_D - V_{DS}) characteristics of In_2O_3 /pentacene TFTs with the first layer thickness (In_2O_3) of 3 nm. As shown in Fig. 2(a), the heterostructure device with In_2O_3 thickness of 3 nm exhibits ambipolar characteristics of both hole accumulation and electron accumulation modes. However, as the thickness of the In_2O_3 layer was increased, the n -channel characteristics were greatly enhanced, whereas the p -channel behavior was diminished (data not shown). These results infer that the first layer thickness and its morphology play a major role in obtaining balanced ambipolar characteristics. The importance of the first layer thickness in achieving the ambipolar transport is also reported in organic heterostructures such as $\text{CuPc}/\text{F}_{16}\text{CuPc}$.¹² Hence, for the realization of the ambipolar behavior of the In_2O_3 /pentacene heterostructure, the critical thickness of In_2O_3 required was found to be 3 nm. For the further elucidation of the transport behavior, the transfer curve was plotted and shown in Fig. 3(a). The field effect mobility and the threshold voltage values were extracted using the relation $I_D = (WC_i\mu_{FE}/2L)(V_{GS} - V_T)^2$

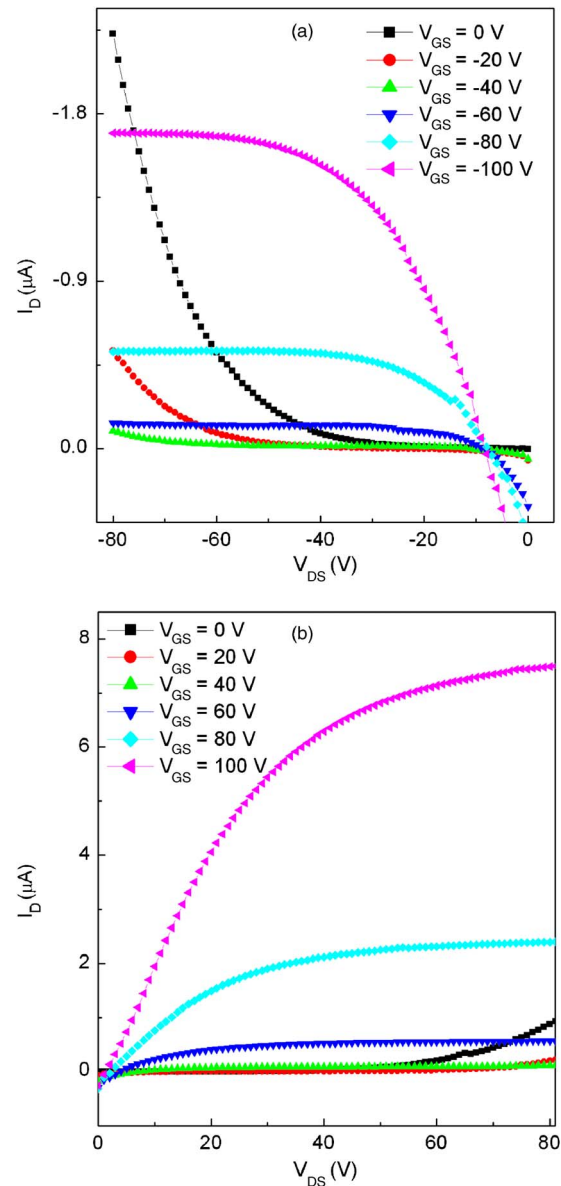


FIG. 2. (Color online) Output curves for the (a) p -channel and (b) n -channel regimes of the ambipolar TFT (V_{GS} ranging from 0 to ± 100 V at a step of ± 20 V).

These ambipolar TFTs exhibited a balanced electron and hole transport, with field effect mobilities of 0.07 and 0.02 $\text{cm}^2/\text{V s}$ for n and p channels, respectively. The corresponding threshold voltages were 38.5 and -35.1 V for the n and p channels. A relatively larger value of threshold voltages for the n -channel devices suggests a significant carrier trapping at the $\text{SiO}_2/\text{In}_2\text{O}_3$ interface. In order to further characterize the transport behavior, their subthreshold voltage swing (S), which is the voltage required to increase the drain current by a factor of 10, was calculated using the relation¹³ $S = [dV_{GS}/d \log(I_{DS})]$, and subsequently, those values were used for the computation of the trapped charge densities at the gate/dielectric interface. The extracted S values for the n - and p -channel regimes were 1.6 and 1.43 V/decade, respectively. The corresponding trapped charges were 1.9×10^{11} and $9.3 \times 10^{10} \text{ cm}^{-2}$. A slightly higher value of the trapped charges at the $\text{In}_2\text{O}_3/\text{SiO}_2$ interface explains the marginal increase in their threshold voltages in the n channel.

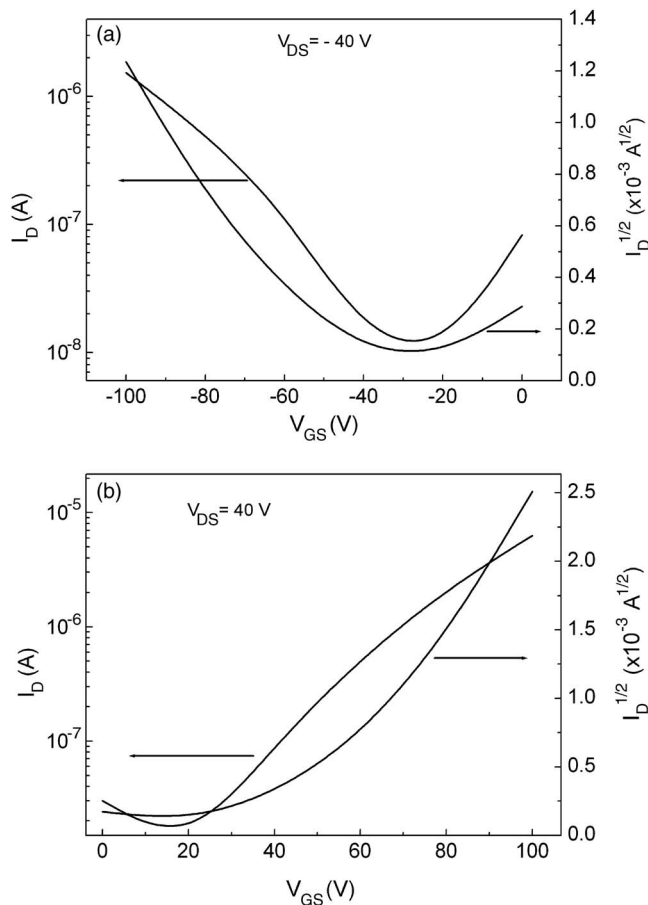


FIG. 3. Transfer curve together with the plot of $I_D^{1/2}$ vs V_{GS} measured at $V_{DS} = \pm 40$ V for (a) p -channel and (b) n -channel regimes of the ambipolar TFT.

In order to further characterize these hybrid ambipolar TFTs, their complementary inverter circuits were constructed using two identical ambipolar TFTs. The schematic of such circuit is displayed in the inset of Figs. 4(a) and 4(b). In the inverter circuit, the gate is common for both transistors and serves as an input node (V_{in}). When the supply voltage (V_{DD}) and the input voltage (V_{in}) are biased positively, the inverter function in the first quadrant, and the output voltage (V_{out}) versus input voltage (V_{in}) plot exhibits a gain of 9. When the V_{DD} and V_{in} are negative, the inverter exhibited a gain of 12, and they function in the third quadrant of the voltage transfer curve. Experimentally measured voltage transfer curve and the corresponding gains for the CMOS-like inverter circuit are displayed in Fig. 4. Hence, it can be observed from the curves that, unlike the p - or n -channel devices, where they operate only in one of the modes, these heterostructures operate in both modes, making the circuit design more simpler.

In summary, we have fabricated ambipolar TFTs through a hybrid route by combining organic/inorganic semiconductors. Both n channel and p channel behaviors of the ambipolar TFTs were analyzed together with their corresponding inverter circuits. A balanced field effect mobility for both n and p channels of 0.07 and 0.02 cm^2/Vs was obtained. Relatively larger threshold voltages and the higher hysteresis in the n channel suggest that carrier trapping for the electrons is higher than that for holes. Overall, $\text{In}_2\text{O}_3/\text{pentacene}$ heterostructure exhibits an ambipolar be-

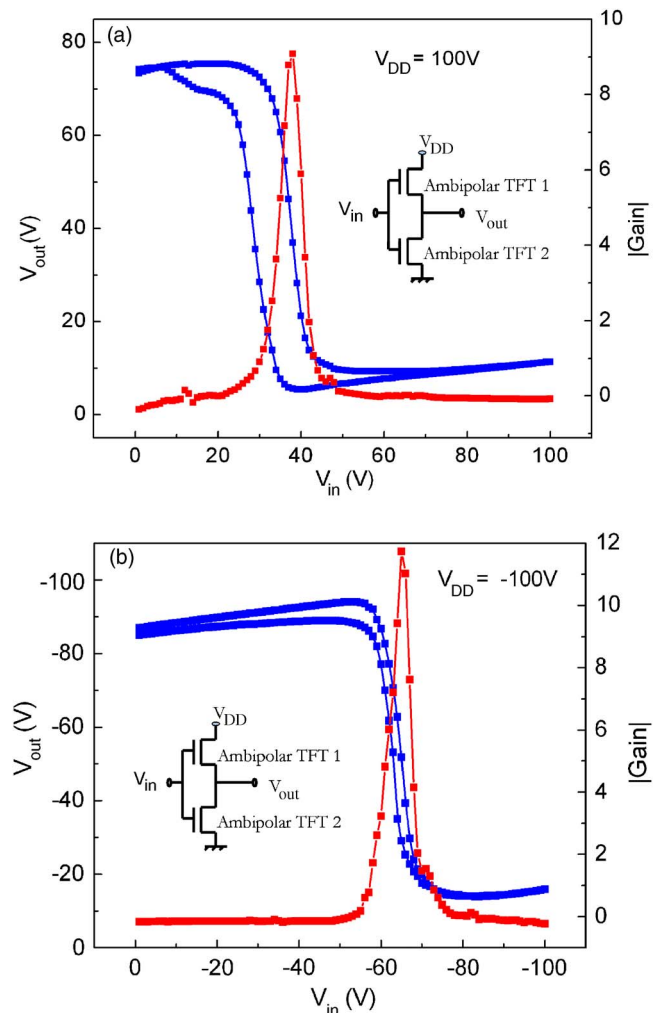


FIG. 4. (Color online) Voltage transfer curve and their corresponding gains of ambipolar TFTs operated in the (a) first quadrant and (b) third quadrant (inset: inverter circuit comprising of two identical TFTs).

havior with balanced field effect mobilities and qualifies them as promising candidates for the applications in CMOS technology.

- ¹T. Sakanoue, M. Yahiro, C. Adachi, H. Uchiuzou, T. Takahashi, and A. Tshimitsu, *Appl. Phys. Lett.* **90**, 171118 (2007).
- ²M. M. Ling, Z. Bao, P. Erk, M. Koenemann, and M. Gomez, *Appl. Phys. Lett.* **90**, 093508 (2007).
- ³Th. B. Singh, P. Senkarabacak, N. S. Sariciftci, A. Tanda, C. Lackner, and R. Hagelauer, *Appl. Phys. Lett.* **89**, 033512 (2006).
- ⁴Q. Tang, Y. Tong, H. Li, Z. Li, L. Li, W. Hu, Y. Liu, and D. Zhu, *Adv. Mater. (Weinheim, Ger.)* **20**, 1 (2008).
- ⁵E. J. Meijer, D. M. De Leeuw, S. Setayesh, E. Van Veenendaal, B.-H. Huisman, P. W. M. Blom, J. C. Hummelen, U. Scherf, and T. M. Klapwijk, *Nat. Mater.* **2**, 678 (2003).
- ⁶A. Dodabalapur, H. E. Katz, L. Torsi, and R. C. Haddon, *Appl. Phys. Lett.* **68**, 1108 (1996).
- ⁷T. P. I. Saragi and J. Salbeck, *Appl. Phys. Lett.* **89**, 253516 (2006).
- ⁸S.-H. Li, Z. Xu, L. Ma, C.-W. Chu, and Y. Yang, *Appl. Phys. Lett.* **91**, 083507 (2007).
- ⁹T. Yasuda, T. Goto, K. Fujita, and T. Tsutsui, *Appl. Phys. Lett.* **85**, 2098 (2004).
- ¹⁰Dhananjay and C.-W. Chu, *Appl. Phys. Lett.* **91**, 132111 (2007).
- ¹¹Dhananjay, S.-S. Cheng, C.-Y. Yang, C.-W. Ou, Y.-C. Chuang, M. Chyi Wu, and C.-W. Chu, *J. Phys. D* **41**, 092006 (2008).
- ¹²R. Ye, M. Baba, K. Suzuki, and K. Mori, *Jpn. J. Appl. Phys., Part 1* **46**, 2878 (2007).
- ¹³C.-W. Ou, Dhananjay, Z.-Y. Ho, Y.-C. Chuang, S.-S. Cheng, M.-C. Wu, K.-C. Ho, and C.-W. Chu, *Appl. Phys. Lett.* **92**, 122113 (2008).